Locate the parameters of RBF networks using a hybrid Particle Swarm Optimization method

Ioannis G. Tsoulos, Vasilieos Charilogis

Department of Informatics and Telecommunications, University of Ioannina, Greece

Abstract

The present paper proposes a two-phase technique for training RBF neural networks. In the first phase, a hybrid algorithm combining interval techniques and particle swarm optimization is used to detect the initialization interval of the neural network parameters. In the second phase, a hybrid algorithm that conjuncts particle swarm optimization and local minimization is used to train the neural network within the space identified in the first phase. This technique is evaluated on a number of regression and classification datasets from the relevant literature.

1 Introduction

Regression and data classification are two major categories of problems that are solved with machine learning techniques. Such problems appear regularly in scientific areas such as physics [1, 2], chemistry [3, 4], economics [5, 6], medicine [7, 8], etc. A programming tool that is used quite often to handle such problems is the RBF artificial neural network [9]. An RBF networks can be expressed as a function:

$$y(\overrightarrow{x}) = \sum_{i=1}^{k} w_i \phi(\|\overrightarrow{x} - \overrightarrow{c_i}\|) \tag{1}$$

The following applies to the above equation

1. The vector $\overrightarrow{x}$ is the input pattern to the equation. The number of values in this vector is denoted as d.
2. The vectors $\overrightarrow{c_i},\ i = 1, .., k$ are denoted as the center vectors.
3. The vector $\overrightarrow{w}$ is considered as the output weight of the RBF network.
4. The value $y(\overrightarrow{x})$ is the predicted value of the network for the pattern $\overrightarrow{x}$.

Typically, the function $\phi(x)$ is a Gaussian function defined as:

$$\phi(x) = \exp\left(-\frac{(x-c)^2}{\sigma^2}\right) \tag{2}$$

A plot for the Gaussian function with $c = 0,\ \sigma = 1$ is shown in Figure 1. As can be seen from the figure, the value of the function decreases as we move away from the center. An extensive overview of RBF networks is given in the work of Ghosh and Nag [10]. RBF networks are used as approximation tools in various cases, such as solutions of differential equations [11, 12], digital communications [13, 14], physics [15, 16], chemistry [17, 18], economics [19, 20, 21], network security [22, 23] etc. RBF networks are thoroughly discussed in [24] and it has been parallelized in a variety of research papers [25, 26]. This model has been extended by various researchers in tasks such as creating new initialization techniques for the network parameters, [27, 28, 29], pruning techniques [30, 32, 31], construction of RBF networks [33, 34, 35] etc. In the current work, a hybrid technique is proposed for the optimal calculation of the parameters of an RBF network. This technique consists of two phases: during the first phase a range of values for the network parameters is estimated using an interval technique, guided by a Particle Swarm Optimizer (PSO). In the second phase, the network parameters are optimized within the optimal value interval of the first phase using a genetic algorithm.

The rest of this article is organized as follows: in section 2 the two phases of the proposed method are thoroughly discussed, in section 3 the experimental datasets are listed as well as the experimental results and finally in section 4 some conclusions are presented.

2 Method description

The training error of the RBF network is expressed as:

$$E(y(x,g)) = \sum_{i=1}^{m} \left(y\left(x_i, g\right) - t_i\right)^2 \tag{3}$$

where m is the number of patterns and t_i is the output for pattern x_i. The vector g is the set of the parameters of the RBF network. Usually, RBF networks are trained through a two phase procedure:

1. In the first phase the k centers as well as the associated variances are estimated through K-Means algorithm [36]. A typical formulation of the K-Means algorithm is outlined in Algorithm 1.

2. In the second phase, the weight vector $\overrightarrow{w} = (w_1, w_2, \ldots, w_k)$ is estimated by solving a linear system of equations.

   (a) **Set** $W = w_{kj}$

Figure 1: Typical plot for the Gaussian function.

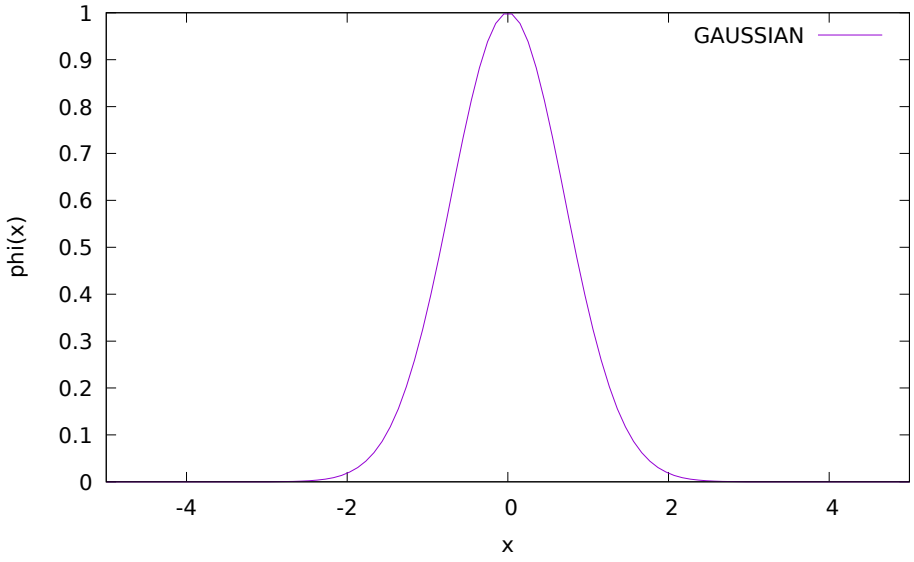

(b) **Set** $\Phi = \phi_j(x_i)$

(c) **Set** $T = \{t_i = f(x_i), i = 1, .., M\}$**.**

(d) The system to be solved is identified as:

$$\Phi^T \left(T - \Phi W^T\right) = 0 \tag{4}$$

With solution:

$$W^T = \left(\Phi^T \Phi\right)^{-1} \Phi^T T = \Phi^\dagger T \tag{5}$$

The proposed work uses two computational phases to optimally calculate the network parameters. In the first phase, a promising range for the parameters of the network is calculated through an optimization process that incorporates interval arithmetic. In the second phase, the parameters of the network are trained with the usage of a genetic algorithm inside the located range of the first phase. The following subsections analyze both of these phases in detail.

2.1 Preliminaries

In order to perform interval arithmetic on RBF networks the following definitions are introduced:

1. The comparison of two intervals $W = [w_1, w_2]$, $Z = [z_1, z_2]$ is performed through the function

$$L^*(W, Z) = \begin{cases} \text{TRUE}, & w_1 < z_1, \text{OR } (w_1 = z_1 \text{ AND } w_2 < z_2) \\ \text{FALSE}, & \text{OTHERWISE} \end{cases} \tag{6}$$

Algorithm 1 The K-Means algorithm.

1. **Repeat**
   (a) $S_j = \{\},\ j = 1..k$
   (b) **For** each sample $x_i,\ i = 1, ..., m$ **Do**
      i. **Calculate** $j^* = \min_{i=1}^{k} \{D(x_i, c_j)\}$, the nearest center for sample x_i.
      ii. **Set** $S_{j^*} = S_{j^*} \cup \{x_i\}$.
   (c) **EndFor**
   (d) **For** every center $c_j,\ j = 1..k$ **Do**
      i. **Define** M_j as the number of elements in S_j
      ii. **Calculate** c_j

$$c_j = \frac{1}{M_j} \sum_{i=1}^{M_j} x_i$$

   (e) **EndFor**

2. **Calculate** the variances for every center as

$$s_j^2 = \frac{\sum_{i=1}^{M_j} (x_i - c_j)^2}{M_j}$$

3. **Terminate** if there is no change in centers c_j.

2. The function $E(y)$ (equation 3) is modified to an interval one

$$[E_{min}, E_{max}] = \sum_{i=1}^{M} \left(y\left(x_i\right) - t_i\right)^2 \tag{7}$$

In the proposed algorithm, the RBF network contains n variables, where

$$n = (d+2) \times k \tag{8}$$

The value of n is calculated as follows:

1. Every center $\overrightarrow{c_i},\ i = 1, .., k$ has d variables, which means $d \times k$ variables.
2. For every center a separated value σ_i is used for the Gaussian processing unit, which means k variables.
3. The output weight $\overrightarrow{w}$ has also k variables.

2.2 The proposed PSO algorithm

During this phase, arithmetic interval techniques are used to find a suitable range for the parameters of the RBF network. The interval techniques [37, 38, 39] are a common method in global optimization with various applications [40, 41, 42]. The first phase aims to locate the most promising bounding box for the n parameters of the neural network. The initial bounding box is defined as S which is a subset of $\mathbb{R}^{\mathrm{n}}$:

$$S = [a_1, b_1] \otimes [a_2, b_2] \otimes \ldots [a_n, b_n] \tag{9}$$

The interval method of the first phase divides the set S subsequently by discarding areas that may not contain the global optimum of equation 3. In order to locate the best interval for the parameters of the network, a modified PSO algorithm [43] is used, in which the particles are intervals for the network parameters. The PSO method is a global optimization method based on a population of candidate solutions, that in most cases called particles. The method is based on two vectors: the current location of particles denoted as $\overrightarrow{p}$ and the velocity of their movement denoted as $\overrightarrow{u}$. The PSO method finds the global minimum by moving the particles based on their previous best position as well as the best position of the total population of particles.

The initial bounding boxes for the centers and variances of the RBF network are constructed using the K-Means clustering algorithm. Subsequently, the initial values for the intervals $[a_i, b_i]$ are calculated through the algorithm 2. The values for the intervals of the first $(d+1) \times k$ variables are obtained as a multiple of the positive quantity F with the values obtained by the K-Means. The value B is used to initialize the intervals for the output weight $\overrightarrow{w}$. Afterwards, the following PSO variant is executed:

1. **Set** N_c the number of particles.

2. **Set** the normalization factor λ.
3. **Set** the k weights of the RBF network.
4. **Set** N_g the maximum number of generations allowed.
5. **Set** N_s the number of random samples that will be used in the fitness calculation algorithm.
6. **Set** $f^* = [\infty, \infty]$, the fitness of the best located particle p^*.
7. **Construct** $S = [a_1, b_1] \otimes [a_2, b_2] \otimes \ldots [a_n, b_n]$, as obtained from the previous two algorithms.
8. **Initialize** the N_g particles. Each particle $p_i,\ i = 1, ..., N_c$ is considered as a set of intervals randomly initialized in S. The layout of each chromosome is graphically presented in Figure 2.
9. **For** $i = 1, ..., N_c$ **do**
   (a) **Calculate** the fitness f_i of particle p_i using the procedure outlined in Algorithm 3.
   (b) **If** $L^*(f_i, f^*) = \text{TRUE}$ **then** $f^* = f_i,\ p^* = p_i$
   (c) **Set** $p_{b,i} = p_i,\ f_{b,i} = f_i$ the best located position for particle i and the associated fitness value.
   (d) **For** $j = 1, ..., n$ do
      i. **Set** δ the width of interval p_{ij}
      ii. **Set** $u_{ij} = \left[-r\frac{\delta}{20}, r\frac{\delta}{20}\right]$, where r a random number in $[0, 1]$.
   (e) **EndFor**
10. **EndFor**
11. **Set** iter=0
12. **Calculate** the inertia value as $\omega = \omega_{\max} - \frac{\text{iter}}{N_g}(\omega_{\max} - \omega_{\min})$where common values for these parameters are $\omega_{\min} = 0.4$ and $\omega_{\max} = 0.9$
13. **For** $i = 1, ..., N_c$ **do**
   (a) **Calculate** the new velocity $u_i = \omega u_i + r_1(p_{b,i} - p_i) + r_2(p^* - p_i)$
   (b) **Normalize** the velocity as: $u_i = \frac{1}{\lambda}u_i$, where λ a positive number with $\lambda > 1$.
   (c) **Update** the position $p_i = p_i + u_i$
   (d) **Calculate** the fitness f_i of particle p_i
   (e) **If** $L^*(f_i, f_{b,i}) = \text{TRUE}$ **then** $p_{b,i} = p_i,\ f_{b,i} = f_i$
   (f) **If** $L^*(f_i, f^*) = \text{TRUE}$ **then** $f^* = f_i,\ p^* = p_i$

Algorithm 2 The location of the initial values for $[a_i, b_i]$, $i = 1, ..., n$

1. **Set** m=0
2. **Set** $F > 1,\ B > 0$
3. **For** $i = 1..k$ **do**
   (a) **For** $j = 1..d$ **do**
      i. **Set** a_m=$-F \times c_{ij}$, b_m=$F \times c_{ij}$
      ii. **Set** $m = m + 1$
   (b) **EndFor**
   (c) **Set** $a_m = -F \times \sigma_i$, $b_m = F \times \sigma_i$
   (d) **Set** $m = m + 1$
4. **EndFor**
5. **For** $j = 1, ..., k$ **do**
   (a) **Set** $a_m = -B,\ b_m = B$
   (b) **Set** $m = m + 1$
6. **EndFor**

Figure 2: The layout of the particles in the proposed PSO algorithm.

c_{11}	c_{12}	...	c_{1d}	σ_1	c_{21}	c_{22}	...	c_{2d}	σ_2	...	c_{k1}	c_{k2}	...	c_{kd}	σ_k	w_1	w_2	...	w_k

14. **EndFor**
15. **Set** iter=iter+1
16. **If** iter$\leq N_g$ goto step 13.
17. **Else Return** $S = [a_1, b_1] \otimes [a_2, b_2] \otimes \ldots [a_n, b_n]$ the domain range for the best particle p^*.

2.3 Optimization of parameters through genetic algorithm

In the second phase of the proposed method, a genetic algorithm is performed, which optimizes the parameters of the RBF network within the optimal interval calculated in the first phase. The used genetic algorithm has its roots in the GA (c_{r1}, l) algorithm from the paper of Kaelo and Ali [44]. This method is enhanced using the stopping rule suggested by Tsoulos [45]. This genetic algorithm has the following steps:

1. **Initialization Step**

Algorithm 3 Fitness calculation for the modified PSO algorithm.

The fitness calculation for a given particle g has as follows:

1. **Take** N_S random samples in g.
2. **Calculate** $E_{\min}(g) = \min_{g_i \in N_S} \left(\left(\sum_{j=1}^{M} y(x_j, g_i) - t_j \right)^2 \right)$.
3. **Calculate** $E_{max}(g) = \max_{g_i \in N_S} \left(\left(\sum_{j=1}^{M} y(x_j, g_i) - y_j \right)^2 \right)$
4. **Return** $f_g = [E_{min}(g), E_{max}(g)]$.

(a) **Set** as N_c the number of chromosomes. Every chromosome is coded as in case of PSO using the scheme of Figure 2.

(b) **Set** as N_g the maximum number of generations allowed.

(c) **Set** k the number of nodes for the RBF network.

(d) **Obtain** the domain range S from the procedure of subsection 2.2.

(e) **Initialize** the N_C randomly in S.

(f) **Set** the selection rate $p_s \in [0, 1]$

(g) **Set** the mutation rate $p_m \in [0, 1]$

(h) **Set** iter=0

2. **Evaluation Step**

   For every chromosome g **calculate** the associated fitness value $f_g = \sum_{i=1}^{m} (y(x_i, g) - t_i)^2$

3. **Genetic operations step**

   Apply the genetic operations of selection, crossover and mutation.

   (a) **Selection procedure.** First, chromosomes are sorted based on their fitness value. The first $(1 - p_s) \times N_c$ with the best fitness value are transferred unchanged to the next generation, and the rest are replaced by offspring resulting from crossover. During the crossover procedure, a series of mating pairs are selected using the well - known procedure of tournament selection for every parent. The tournament selection is formulated as:

      i. The algorithm selects a set of $T > 2$ chromosomes from the population

      ii. The chromosome with the best fitness value in the set is selected as the mating parent.

(b) **Crossover procedure** : For every pair (z, w) of parents two offsprings $\tilde{z}$ and $\tilde{w}$ are created as:

$$\begin{aligned} \tilde{z}_i &= a_i z_i + (1 - a_i) w_i \\ \tilde{w}_i &= a_i w_i + (1 - a_i) z_i \end{aligned} \tag{10}$$

with a_i being a random number with the property $a_i \in [-0.5, 1.5]$ [44].

(c) **Mutation procedure** : Draw a random number $r \in [0, 1]$ for each element of every chromosome. IF $r \leq p_m$, then the corresponding element is altered randomly.

4. **Termination Check Step**
   (a) **Set** $iter = iter + 1$
   (b) **Terminate** if the termination criteria are satisfied, **else Goto** Evaluation Step.

3 Experiments

The proposed method was tested on a series of classification and regression problems found in various papers and sites from the relevant literature. For the classification problems two internet databases were used:

1. The UCI dataset repository, `https://archive.ics.uci.edu/ml/index.php`
2. The Keel repository, `https://sci2s.ugr.es/keel/datasets.php`[46].

The regression datasets was found in the Statlib URL `ftp://lib.stat.cmu.edu/datasets/index.html`.

3.1 Experimental datasets

The following classification datasets were used:

1. **Appendictis** dataset, a medical dataset suggested in [47].
2. **Australian** dataset [48], which is related to credit card applications.
3. **Balance** dataset [49], used for prediction of psychological states.
4. **Cleveland** dataset, a dataset related to heart diseases [50, 51].
5. **Bands** dataset, a dataset related to printing problems [52].
6. **Dermatology** dataset [53], which is a medical dataset.
7. **Hayes roth** dataset. This dataset[54] contains **5** numeric-valued attributes and 132 patterns.

8. **Heart** dataset [55], a medical dataset about heart diseases.
9. **HouseVotes** dataset [56], which is about votes in the U.S. House of Representatives Congressmen.
10. **Ionosphere** dataset a dataset found the Johns Hopkins database [57, 58].
11. **Liverdisorder** dataset [59], a medical dataset about liver disorders.
12. **Lymography** dataset [60]. The aim here is to detect the presence of a lymphoma in patients.
13. **Mammographic** dataset [61], which is a dataset about breast cancer.
14. **Parkinsons** dataset. This dataset is composed of a range of biomedical voice measurements from 31 people, 23 with Parkinson's disease (PD)[62].
15. **Pima** dataset, a medical dataset used to predict cases of diabetes [63].
16. **Popfailures** dataset [64], a dataset about climate.
17. **Spiral** dataset: The spiral artificial dataset contains 1000 two-dimensional examples that belong to two classes (500 examples each). The number of the features is 2. The data in the first class are created using the following formula: $x_1 = 0.5t\cos(0.08t)$, $x_2 = 0.5t\cos\left(0.08t + \frac{\pi}{2}\right)$ and the second class data using**:** $x_1 = 0.5t\cos(0.08t + \pi)$, $x_2 = 0.5t\cos\left(0.08t + \frac{3\pi}{2}\right)$
18. **Regions2** dataset. It is created from liver biopsy images of patients with hepatitis C [65].
19. **Saheart** dataset [66], which is related to heart diseases.
20. **Segment** dataset [67], which is related to image processing.
21. **Wdbc** dataset [68], which is related to breast tumors.
22. **Wine** dataset. The wine recognition dataset contains data from wine chemical analysis. It contains 178 examples of 13 features each that are classified into three classes. It has been examinated in various research papers [69, 70].
23. **Eeg** dataset. As an real word example, consider an EEG dataset described in [71] is used here. The datasets derived from the dataset are denoted as Z_F_S, ZONF_S and ZO_NF_S.
24. **Zoo** dataset [72], where the task is classify animals in seven predefined classes.

The regression datasets are:

1. **Abalone** dataset [73]. This dataset can be used to obtain a model to predict the age of abalone from physical measurements.

2. **Airfoil** dataset, a dataset from NASA related to aerodynamic and acoustic tests [74].

3. **Baseball** dataset, a dataset used to predict the outcome of baseball players.

4. **BK** dataset [75] and is used to estimate the points scored per minute in a basketball game.

5. **BL** dataset, this dataset is related to an experiment on the affects of machine adjustments on the time to count bolts.

6. **Concrete** dataset. This dataset is taken from civil engineering[76].

7. **Dee** dataset, used to predict the daily average price of the electricity energy in Spain.

8. **Diabetes** dataset, a medical dataset.

9. **FA** dataset, which is related to fat measurements.

10. **Housing** dataset. This dataset was taken from the StatLib library and it is described in [77].

11. **MB** dataset. This dataset is available from Smoothing Methods in Statistics [78] and it includes 61 patterns.

12. **MORTGAGE** dataset, which contains the Economic data information of USA.

13. **NT** dataset, derived from [79].

14. **PY** dataset (Pyrimidines problem)[80].

15. **Quake** dataset. The objective here is to approximate the strength of a earthquake [81].

16. **Treasure** dataset, which contains Economic data information of USA

17. **Wankara** dataset, which contains weather measurements.

3.2 Experimental results

The RBF network for the experiments was coded in ANSI C++ with the help of the freely available Armadillo library [82]. In addition, in order to have greater reliability in the experimental results, a 10-fold validation technique was used. All the experiments were executed 30 times with different seeds for the random generator each time and average was measured. For the classification datasets the average classification error was reported and for the regression datasets the mean test error. All the experiments were conducted on an AMD Ryzen 5950X equipped with 128GB of RAM. The operating system used was Debian Linux. In

order to speed up the training process, the OpenMP library was incorporated [83]. The experimental settings are listed in the Table 1. The experimental results for the classification datasets are listed in Table 2and for the regression datasets in Table 3. The following applies to the tables of results:

1. The column RBF-KMEANS denotes the classic training method for RBF networks by estimating centers and variances through K-Means and the output weights by solving a linear system of equations.
2. The column IRBF-100 denotes the application of the proposed method with $\lambda = 100$.
3. The column IRBF-1000 denotes the application of the proposed method with $\lambda = 1000$.
4. In both tables an extra line has been added, in which the mean error for each method is shown. This row is denoted by the name AVERAGE.

From the experimental results, it is evident that the proposed technique significantly outperforms the RBF training technique by an average of 35-40% in terms of error in the test set. In fact, in some datasets this gain is more than doubled. Furthermore, the differences in performance between the original training method and the proposed technique are graphically presented in the figures 3 and 4. However, the proposed technique is significantly slower than the original training technique, as it is a two-stage technique. In the first stage, an optimal interval of values for the network parameters is created with a modified PSO method, and in the second stage, the network is trained using a genetic algorithm. Of course, this extra time could be significantly reduced by using parallel techniques, as was done experimentally using the OpenMP library. Furthermore, changing the normalization factor λ from 100 to 1000 did not have much effect on the mean error in the test set. This means that the proposed method is quite robust, since it doesn't have much dependence on this parameter.

An additional experiment was performed with different values for the parameter F. The results for the classification data are presented in Table 4, and the results for the regression problems in Table 5. And for this critical parameter, no large deviations appear in the results of the proposed method. This further enhances the robustness and reliability of the proposed technique.

4 Conclusions

In this work, a two-stage technique for data classification and function regression was presented using an RBF model. In the first stage of the technique, an attempt is made to discover a promising range of values for the network parameters and, in the second stage, the network parameters are adjusted within this range using a genetic algorithm. From the experiments performed, it appears that this technique is in most cases much more efficient than the traditional

Table 1: Experimental parameters

PARAMETER	VALUE
N_c	200
N_g	100
N_s	50
F	5.0
B	100.0
k	10
p_s	0.90
p_m	0.05

Table 2: Experiments for classification datasets

DATASET	RBF-KMEANS	IRBF-100	IRBF-1000
Appendicitis	12.23%	16.47%	14.03%
Australian	34.89%	23.61%	22.39%
Balance	33.42%	12.65%	13.15%
Bands	37.22%	37.38%	36.29%
Cleveland	67.10%	49.77%	49.64%
Dermatology	62.34%	38.24%	35.64%
Hayes Roth	64.36%	33.62%	34.13%
Heart	31.20%	15.91%	15.60%
HouseVotes	6.13%	4.77%	3.90%
Ionosphere	16.22%	8.64%	7.52%
Liverdisorder	30.84%	27.36%	25.63%
Lymography	25.31%	19.12%	20.02%
Mammographic	21.38%	17.17%	17.30%
Parkinsons	17.41%	15.51%	13.59%
Pima	25.78%	23.61%	23.23%
Popfailures	7.04%	5.21%	5.10%
Regions2	38.29%	26.08%	25.77%
Saheart	32.19%	27.94%	28.91%
Segment	59.68%	47.19%	40.28%
Spiral	44.87%	19.43%	19.56%
Wdbc	7.27%	5.33%	5.44%
Wine	31.41%	9.20%	6.84%
Z_F_S	13.16%	4.19%	4.18%
ZO_NF_S	9.02%	4.31%	4.35%
ZONF_S	4.03%	2.23%	2.08%
ZOO	21.93%	10.13%	11.13%
AVERAGE	**29.03%**	**19.43%**	**18.68%**

Table 3: Experiments for regression datasets.

DATASET	RBF-KMEANS	IRBF-100	IRBF-1000
ABALONE	7.37	5.57	5.32
AIRFOIL	0.27	0.004	0.003
BASEBALL	93.02	78.89	85.58
BK	0.02	0.04	0.03
BL	0.013	0.0003	0.0003
CONCRETE	0.011	0.007	0.007
DEE	0.17	0.16	0.16
DIABETES	0.49	0.78	0.89
HOUSING	57.68	20.27	21.54
FA	0.015	0.032	0.029
MB	2.16	0.12	0.09
MORTGAGE	1.45	0.39	0.78
NT	8.14	0.007	0.007
PY	0.012	0.024	0.014
QUAKE	0.07	0.04	0.03
TREASURY	2.02	0.33	0.51
WANKARA	0.001	0.002	0.002
AVERAGE	**10.17**	**6.27**	**6.76**

Figure 3: Graphical comparison of the three methods for the classification datasets.

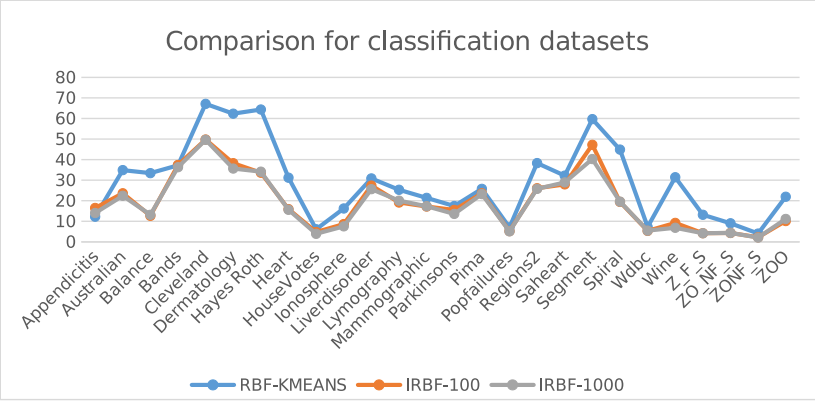

Table 4: Experimental results using different values for the parameter F on the classification datasets.

DATASET	$F = 3$	$F = 5$	$F = 10$
Appendicitis	14.43%	14.03%	14.47%
Australian	23.45%	22.39%	23.21%
Balance	13.35%	13.15%	11.79%
Bands	36.48%	36.29%	36.76%
Cleveland	49.26%	49.64%	49.02%
Dermatology	36.54%	35.64%	34.37%
Hayes Roth	39.28%	34.13%	36.46%
Heart	15.14%	15.60%	14.89%
HouseVotes	4.93%	3.90%	6.41%
Ionosphere	7.56%	7.52%	9.05%
Liverdisorder	28.37%	25.63%	28.97%
Lymography	20.12%	20.02%	21.05%
Mammographic	18.04%	17.30%	18.21%
Parkinsons	18.51%	13.59%	13.49%
Pima	23.69%	23.23%	23.52%
Popfailures	5.76%	5.10%	4.50%
Regions2	25.79%	25.77%	25.32%
Saheart	28.89%	28.91%	26.99%
Segment	36.53%	40.28%	43.28%
Spiral	16.78%	19.56%	22.18%
Wdbc	4.64%	5.44%	5.10%
Wine	8.31%	6.84%	8.27%
Z_F_S	4.32%	4.18%	4.03%
ZO_NF_S	3.70%	4.35%	3.72%
ZONF_S	2.04%	2.08%	1.98%
ZOO	11.87%	11.13%	9.97%
AVERAGE	**18.65%**	**18.68%**	**19.12%**

Figure 4: Graphical comparison of the methods for the regression datasets.

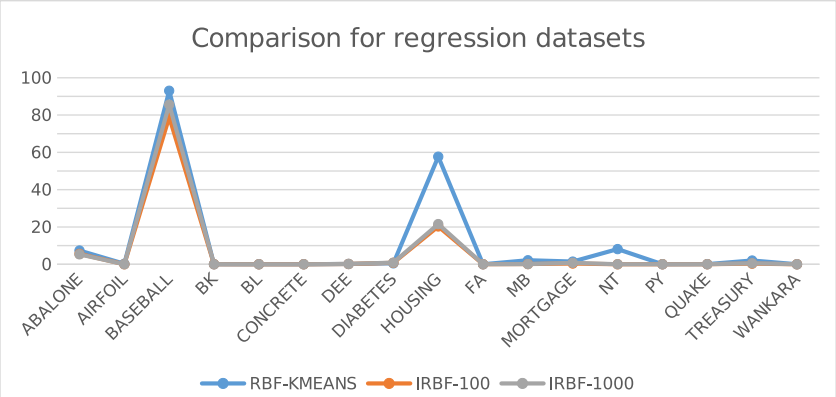

Table 5: Experimental results using different values for the parameter F on the classification datasets.

DATASET	$F = 3$	$F = 5$	$F = 10$
ABALONE	5.56	5.32	5.41
AIRFOIL	0.004	0.003	0.004
BASEBALL	88.40	85.58	84.43
BK	0.03	0.03	0.02
BL	0.0005	0.0003	0.0002
CONCRETE	0.009	0.007	0.007
DEE	0.18	0.16	0.16
DIABETES	0.67	0.89	0.77
HOUSING	20.03	21.54	20.84
FA	0.03	0.029	0.036
MB	0.19	0.09	0.26
MORTGAGE	0.89	0.78	0.03
NT	0.006	0.007	0.007
PY	0.027	0.014	0.018
QUAKE	0.04	0.03	0.04
TREASURY	0.77	0.51	0.17
WANKARA	0.002	0.002	0.002
AVERAGE	**6.87**	**6.76**	**6.60**

training technique of such models. Moreover, this technique appears to be largely robust, as changes in its critical parameters do not entail large changes in its reliability. However, the proposed technique is significantly more time-consuming than the traditional training technique as it requires computational time for both its phases. However, this problem can be mitigated to a significant extent by the use of modern parallel computing techniques.

References

[1] M. Mjahed, The use of clustering techniques for the classification of high energy physics data, Nuclear Instruments and Methods in Physics Research Section A: Accelerators, Spectrometers, Detectors and Associated Equipment **559**, pp. 199-202, 2006.

[2] M Andrews, M Paulini, S Gleyzer, B Poczos, End-to-End Event Classification of High-Energy Physics Data, Journal of Physics: Conference Series **1085**, 2018.

[3] P. He, C.J. Xu, Y.Z. Liang, K.T. Fang, Improving the classification accuracy in chemistry via boosting technique, Chemometrics and Intelligent Laboratory Systems 70, pp. 39-46, 2004.

[4] J.A. Aguiar, M.L. Gong, T.Tasdizen, Crystallographic prediction from diffraction and chemistry data for higher throughput classification using machine learning, Computational Materials Science **173**, 109409, 2020.

[5] I. Kaastra, M. Boyd, Designing a neural network for forecasting financial and economic time series, Neurocomputing **10**, pp. 215-236, 1996.

[6] R. Hafezi, J. Shahrabi, E. Hadavandi, A bat-neural network multi-agent system (BNNMAS) for stock price prediction: Case study of DAX stock price, Applied Soft Computing **29**, pp. 196-210, 2015.

[7] S.S. Yadav, S.M. Jadhav, Deep convolutional neural network based medical image classification for disease diagnosis. J Big Data **6**, 113, 2019.

[8] L. Qing, W. Linhong , D. Xuehai, A Novel Neural Network-Based Method for Medical Text Classification, Future Internet **11**, 255, 2019.

[9] J. Park and I. W. Sandberg, Universal Approximation Using Radial-Basis-Function Networks, Neural Computation **3**, pp. 246-257, 1991.

[10] J. Ghosh, A. Nag, An Overview of Radial Basis Function Networks. In: Howlett, R.J., Jain, L.C. (eds) Radial Basis Function Networks 2. Studies in Fuzziness and Soft Computing, vol 67. Physica, Heidelberg, 2001.

[11] Nam Mai-Duy, Thanh Tran-Cong, Numerical solution of differential equations using multiquadric radial basis function networks, Neural Networks 14, pp. 185-199, 2001.

[12] N. Mai-Duy, Solving high order ordinary differential equations with radial basis function networks. Int. J. Numer. Meth. Engng. **62**, pp. 824-852, 2005.

[13] C. Laoudias, P. Kemppi and C. G. Panayiotou, Localization Using Radial Basis Function Networks and Signal Strength Fingerprints in WLAN, GLOBECOM 2009 - 2009 IEEE Global Telecommunications Conference, Honolulu, HI, 2009, pp. 1-6, 2009.

[14] M. Azarbad, S. Hakimi, A. Ebrahimzadeh, Automatic recognition of digital communication signal, International journal of energy, information and communications **3**, pp. 21-33, 2012.

[15] P. Teng, Machine-learning quantum mechanics: Solving quantum mechanics problems using radial basis function networks, Phys. Rev. E **98**, 033305, 2018.

[16] R. Jovanović, A. Sretenovic, Ensemble of radial basis neural networks with K-means clustering for heating energy consumption prediction, FME Transactions **45**, pp. 51-57, 2017.

[17] D.L. Yu, J.B. Gomm, D. Williams, Sensor fault diagnosis in a chemical process via RBF neural networks, Control Engineering Practice **7**, pp. 49-55, 1999.

[18] V. Shankar, G.B. Wright, A.L. Fogelson, R.M. Kirby, A radial basis function (RBF) finite difference method for the simulation of reaction–diffusion equations on stationary platelets within the augmented forcing method, Int. J. Numer. Meth. Fluids **75**, pp. 1-22, 2014.

[19] W. Shen, X. Guo, C. Wu, D. Wu, Forecasting stock indices using radial basis function neural networks optimized by artificial fish swarm algorithm, Knowledge-Based Systems 24, pp. 378-385, 2011.

[20] J. A. Momoh, S. S. Reddy, Combined Economic and Emission Dispatch using Radial Basis Function, 2014 IEEE PES General Meeting | Conference & Exposition, National Harbor, MD, pp. 1-5, 2014.

[21] P. Sohrabi, B. Jodeiri Shokri, H. Dehghani, Predicting coal price using time series methods and combination of radial basis function (RBF) neural network with time series. Miner Econ 2021.

[22] U. Ravale, N. Marathe, P. Padiya, Feature Selection Based Hybrid Anomaly Intrusion Detection System Using K Means and RBF Kernel Function, Procedia Computer Science **45**, pp. 428-435, 2015.

[23] M. Lopez-Martin, A. Sanchez-Esguevillas, J. I. Arribas, B. Carro, Network Intrusion Detection Based on Extended RBF Neural Network With Offline Reinforcement Learning, IEEE Access **9**, pp. 153153-153170, 2021.

[24] H. Yu, T. Xie, S. Paszczynski and B. M. Wilamowski, Advantages of Radial Basis Function Networks for Dynamic System Design,IEEE Transactions on Industrial Electronics v **58**, pp. 5438-5450, 2011.

[25] R. Yokota, L.A. Barba, M. G. Knepley, PetRBF — A parallel O(N) algorithm for radial basis function interpolation with Gaussians, Computer Methods in Applied Mechanics and Engineering **199**, pp. 1793-1804, 2010.

[26] C. Lu, N. Ma, Z. Wang, Fault detection for hydraulic pump based on chaotic parallel RBF network, EURASIP J. Adv. Signal Process. **2011**, 49, 2011.

[27] L.I. Kuncheva, Initializing of an RBF network by a genetic algorithm, Neurocomputing **14**, pp. 273-288, 1997.

[28] F. Ros, M. Pintore, A. Deman, J.R. Chrétien, Automatical initialization of RBF neural networks, Chemometrics and Intelligent Laboratory Systems **87**, pp. 26-32, 2007.

[29] D. Wang, X.J. Zeng, J.A. Keane, A clustering algorithm for radial basis function neural network initialization, Neurocomputing **77**, pp. 144-155, 2012.

[30] E. Ricci, R. Perfetti, Improved pruning strategy for radial basis function networks with dynamic decay adjustment, Neurocomputing **69**, pp. 1728-1732, 2006.

[31] Guang-Bin Huang, P. Saratchandran and N. Sundararajan, A generalized growing and pruning RBF (GGAP-RBF) neural network for function approximation, IEEE Transactions on Neural Networks **16**, pp. 57-67, 2005.

[32] M. Bortman and M. Aladjem, A Growing and Pruning Method for Radial Basis Function Networks, IEEE Transactions on Neural Networks **20**, pp. 1039-1045, 2009.

[33] N. B. Karayiannis, M. M. Randolph-Gips, On the construction and training of reformulated radial basis function neural networks, IEEE Transactions on Neural Networks **14**, pp. 835-846, 2003.

[34] J.X. Peng, K. Li, D.S. Huang, A Hybrid Forward Algorithm for RBF Neural Network Construction, IEEE Transactions on Neural Networks, **17**, pp. 1439-1451, 2006.

[35] D. Du, K. Li, M. Fei, A fast multi-output RBF neural network construction method, Neurocomputing **73**, pp. 2196-2202, 2010.

[36] J. MacQueen, Some methods for classification and analysis of multivariate observations, in: Proceedings of the fifth Berkeley symposium on mathematical statistics and probability, Vol. 1, No. 14, pp. 281-297, 1967.

[37] E. Hansen and G.W. Walster.Global Optimization using Interval Analysis.Marcel Dekker Inc., New York, 2004.

[38] M.Cs. Markót,FernándezL.G. and CasadoT. Csendes, New interval methods for constrained global optimization, Mathematical Programming **106**, pp. 287-318, 2006.

[39] A. Žilinskas, and J. Žilinskas, Interval Arithmetic Based Optimization in Nonlinear Regression, Informatica **21**, pp. 149-158, 2010.

[40] C.A. Schnepper, M.A. Stadtherr, Robust process simulation using interval methods, Computers & Chemical Engineering **20**, pp. 187-199, 1996.

[41] C. Carreras, I. D. Walker, Interval methods for fault-tree analysis in robotics, IEEE Transactions on Reliability **50**, pp. 3-11, 2001.

[42] A. Serguieva, J. Hunte, Fuzzy interval methods in investment risk appraisal, Fuzzy Sets and Systems **142**, pp. 443-466, 2004.

[43] Riccardo Poli, James Kennedy kennedy, Tim Blackwell, Particle swarm optimization An Overview, Swarm Intelligence **1**, pp 33-57, 2007.

[44] P. Kaelo, M.M. Ali, Integrated crossover rules in real coded genetic algorithms, European Journal of Operational Research **176**, pp. 60-76, 2007.

[45] I.G. Tsoulos, Modifications of real code genetic algorithm for global optimization, Applied Mathematics and Computation **203**, pp. 598-607, 2008.

[46] J. Alcalá-Fdez, A. Fernandez, J. Luengo, J. Derrac, S. García, L. Sánchez, F. Herrera. KEEL Data-Mining Software Tool: Data Set Repository, Integration of Algorithms and Experimental Analysis Framework. Journal of Multiple-Valued Logic and Soft Computing 17, pp. 255-287, 2011.

[47] Weiss, Sholom M. and Kulikowski, Casimir A., Computer Systems That Learn: Classification and Prediction Methods from Statistics, Neural Nets, Machine Learning, and Expert Systems, Morgan Kaufmann Publishers Inc, 1991.

[48] J.R. Quinlan, Simplifying Decision Trees. International Journal of Man-Machine Studies **27**, pp. 221-234, 1987.

[49] T. Shultz, D. Mareschal, W. Schmidt, Modeling Cognitive Development on Balance Scale Phenomena, Machine Learning **16**, pp. 59-88, 1994.

[50] Z.H. Zhou,Y. Jiang, NeC4.5: neural ensemble based C4.5," in IEEE Transactions on Knowledge and Data Engineering **16**, pp. 770-773, 2004.

[51] R. Setiono , W.K. Leow, FERNN: An Algorithm for Fast Extraction of Rules from Neural Networks, Applied Intelligence **12**, pp. 15-25, 2000.

[52] B. Evans, D. Fisher, Overcoming process delays with decision tree induction, IEEE Expert **9**, pp. 60-66, 1994.

[53] G. Demiroz, H.A. Govenir, N. Ilter, Learning Differential Diagnosis of Eryhemato-Squamous Diseases using Voting Feature Intervals, Artificial Intelligence in Medicine. **13**, pp. 147–165, 1998.

[54] B. Hayes-Roth, B., F. Hayes-Roth. Concept learning and the recognition and classification of exemplars. Journal of Verbal Learning and Verbal Behavior **16**, pp. 321-338, 1977.

[55] I. Kononenko, E. Šimec, M. Robnik-Šikonja, Overcoming the Myopia of Inductive Learning Algorithms with RELIEFF, Applied Intelligence **7**, pp. 39–55, 1997

[56] R.M. French, N. Chater, Using noise to compute error surfaces in connectionist networks: a novel means of reducing catastrophic forgetting, Neural Comput. **14**, pp. 1755-1769, 2002.

[57] J.G. Dy , C.E. Brodley, Feature Selection for Unsupervised Learning, The Journal of Machine Learning Research **5**, pp 845–889, 2004.

[58] S. J. Perantonis, V. Virvilis, Input Feature Extraction for Multilayered Perceptrons Using Supervised Principal Component Analysis, Neural Processing Letters **10**, pp 243–252, 1999.

[59] J. Garcke, M. Griebel, Classification with sparse grids using simplicial basis functions, Intell. Data Anal. **6**, pp. 483-502, 2002.

[60] G. Cestnik, I. Konenenko, I. Bratko, Assistant-86: A Knowledge-Elicitation Tool for Sophisticated Users. In: Bratko, I. and Lavrac, N., Eds., Progress in Machine Learning, Sigma Press, Wilmslow, pp. 31-45, 1987.

[61] M. Elter, R. Schulz-Wendtland, T. Wittenberg, The prediction of breast cancer biopsy outcomes using two CAD approaches that both emphasize an intelligible decision process, Med Phys. **34**, pp. 4164-72, 2007.

[62] Little MA, McSharry PE, Hunter EJ, Spielman J, Ramig LO. Suitability of dysphonia measurements for telemonitoring of Parkinson's disease. IEEE Trans Biomed Eng. 2009;56(4):1015. doi:10.1109/TBME.2008.2005954

[63] J.W. Smith, J.E. Everhart, W.C. Dickson, W.C. Knowler, R.S. Johannes, Using the ADAP learning algorithm to forecast the onset of diabetes mellitus, In: Proceedings of the Symposium on Computer Applications and Medical Care IEEE Computer Society Press, pp.261-265, 1988.

[64] D.D. Lucas, R. Klein, J. Tannahill, D. Ivanova, S. Brandon, D. Domyancic, Y. Zhang, Failure analysis of parameter-induced simulation crashes in climate models, Geoscientific Model Development **6**, pp. 1157-1171, 2013.

[65] Giannakeas, N., Tsipouras, M.G., Tzallas, A.T., Kyriakidi, K., Tsianou, Z.E., Manousou, P., Hall, A., Karvounis, E.C., Tsianos, V., Tsianos, E. A clustering based method for collagen proportional area extraction in liver biopsy images (2015) Proceedings of the Annual International Conference of the IEEE Engineering in Medicine and Biology Society, EMBS, 2015-November, art. no. 7319047, pp. 3097-3100.

[66] T. Hastie, R. Tibshirani, Non-parametric logistic and proportional odds regression, JRSS-C (Applied Statistics) **36**, pp. 260–276, 1987.

[67] M. Dash, H. Liu, P. Scheuermann, K. L. Tan, Fast hierarchical clustering and its validation, Data & Knowledge Engineering **44**, pp 109–138, 2003.

[68] W.H. Wolberg, O.L. Mangasarian, Multisurface method of pattern separation for medical diagnosis applied to breast cytology, Proc Natl Acad Sci U S A. **87**, pp. 9193–9196, 1990.

[69] M. Raymer, T.E. Doom, L.A. Kuhn, W.F. Punch, Knowledge discovery in medical and biological datasets using a hybrid Bayes classifier/evolutionary algorithm. IEEE transactions on systems, man, and cybernetics. Part B, Cybernetics : a publication of the IEEE Systems, Man, and Cybernetics Society, **33** , pp. 802-813, 2003.

[70] P. Zhong, M. Fukushima, Regularized nonsmooth Newton method for multi-class support vector machines, Optimization Methods and Software **22**, pp. 225-236, 2007.

[71] R.G. Andrzejak, K. Lehnertz, F. Mormann, C. Rieke, P. David, and C. E. Elger, Indications of nonlinear deterministic and finite-dimensional structures in time series of brain electrical activity: Dependence on recording region and brain state, Phys. Rev. E **64**, pp. 1-8, 2001.

[72] M. Koivisto, K. Sood, Exact Bayesian Structure Discovery in Bayesian Networks, The Journal of Machine Learning Research **5**, pp. 549–573, 2004.

[73] W. J Nash, T.L. Sellers, S.R. Talbot, A.J. Cawthor, W.B. Ford, The Population Biology of Abalone (_Haliotis_ species) in Tasmania. I. Blacklip Abalone (_H. rubra_) from the North Coast and Islands of Bass Strait, Sea Fisheries Division, Technical Report No. 48 (ISSN 1034-3288), 1994.

[74] T.F. Brooks, D.S. Pope, and A.M. Marcolini. Airfoil self-noise and prediction. Technical report, NASA RP-1218, July 1989.

[75] J.S. Simonoff, Smooting Methods in Statistics, Springer - Verlag, 1996.

[76] I.Cheng Yeh, Modeling of strength of high performance concrete using artificial neural networks, Cement and Concrete Research. **28**, pp. 1797-1808, 1998.

[77] D. Harrison and D.L. Rubinfeld, Hedonic prices and the demand for clean ai, J. Environ. Economics & Management **5**, pp. 81-102, 1978.

[78] J.S. Simonoff, Smooting Methods in Statistics, Springer - Verlag, 1996.

[79] Mackowiak, P.A., Wasserman, S.S., Levine, M.M., 1992. A critical appraisal of 98.6 degrees f, the upper limit of the normal body temperature, and other legacies of Carl Reinhold August Wunderlich. J. Amer. Med. Assoc. 268, 1578–1580

[80] R.D. King, S. Muggleton, R. Lewis, M.J.E. Sternberg, Proc. Nat. Acad. Sci. USA **89**, pp. 11322–11326, 1992.

[81] M. Sikora, L. Wrobel, Application of rule induction algorithms for analysis of data collected by seismic hazard monitoring systems in coal mines, Archives of Mining Sciences **55**, pp. 91-114, 2010.

[82] C. Sanderson, R. Curtin, Armadillo: a template-based C++ library for linear algebra, Journal of Open Source Software **1**, pp. 26, 2016.

[83] R. Chandra, L. Dagum, D. Kohr, D. Maydan,J. McDonald and R. Menon, Parallel Programming in OpenMP, Morgan Kaufmann Publishers Inc., 2001.